
This is an electronic reprint of the original article.
This reprint may differ from the original in pagination and typographic detail.

Tesfaye, Fiseha; Jung, In Ho; Paek, Min Kyu; Moroz, Mykola; Lindberg, Daniel; Hupa, Leena
Thermochemical Data of Selected Phases in the $\text{FeO}_x\text{-FeSO}_4\text{-Fe}_2(\text{SO}_4)_3$ System

Published in:
Materials Processing Fundamentals, 2019

DOI:
[10.1007/978-3-030-05728-2_21](https://doi.org/10.1007/978-3-030-05728-2_21)

Published: 10/02/2019

Document Version
Peer-reviewed accepted author manuscript, also known as Final accepted manuscript or Post-print

Published under the following license:
Unspecified

Please cite the original version:
Tesfaye, F., Jung, I. H., Paek, M. K., Moroz, M., Lindberg, D., & Hupa, L. (2019). Thermochemical Data of Selected Phases in the $\text{FeO}_x\text{-FeSO}_4\text{-Fe}_2(\text{SO}_4)_3$ System. In A. Allanore, G. Lambotte, S. Wagstaff, & J. Lee (Eds.), *Materials Processing Fundamentals*, 2019 (pp. 227-240). (Minerals, Metals and Materials Series). Springer. https://doi.org/10.1007/978-3-030-05728-2_21

This material is protected by copyright and other intellectual property rights, and duplication or sale of all or part of any of the repository collections is not permitted, except that material may be duplicated by you for your research use or educational purposes in electronic or print form. You must obtain permission for any other use. Electronic or print copies may not be offered, whether for sale or otherwise to anyone who is not an authorised user.

Thermochemical Data of Selected Phases in the $\text{FeO}_x\text{--FeSO}_4\text{--Fe}_2(\text{SO}_4)_3$ System



Fiseha Tesfaye, In-Ho Jung, Min-Kyu Paek, Mykola Moroz, Daniel Lindberg and Leena Hupa

Abstract Several recent studies have shown the potential of oxy-fuel combustion to reduce NO_x (gas) and SO_2 (gas) emissions. However, the mechanisms through which SO_2 (gas) reduction takes place has yet to be fully understood. Therefore, the development of oxy-sulfate thermodynamic database for a better understanding and control of SO_2 (gas) emission during oxy-fuel combustion processes is essential. The focus of this research is on the thermodynamic modelling of the iron oxide–sulfate system with the FactSage 7.2 software package. Thermodynamic properties of selected phases in the $\text{FeO}_x\text{--FeSO}_4\text{--Fe}_2(\text{SO}_4)_3$ system were critically reviewed, compiled and assessed over a wide temperature range (298–2000 K) to obtain accurate thermodynamic description of the system at different temperatures. New C_p functions, which include the recent experimental data, were optimized. The obtained results are presented and discussed.

Keywords Sulfate · Sulfur dioxide · Decomposition reaction
Thermochemical data

F. Tesfaye (✉) · M. Moroz · L. Hupa
Laboratory of Inorganic Chemistry, Åbo Akademi University, Johan Gadolin Process Chemistry Centre, Piispankatu 8, 20500 Turku, Finland
e-mail: fiseha.tesfaye@abo.fi

F. Tesfaye · I.-H. Jung · M.-K. Paek
Department of Materials Science and Engineering, Seoul National University, Gwanwak-ro 1, Seoul 08826, Republic of Korea

D. Lindberg
Department of Chemical and Metallurgical Engineering (CMET), School of Chemical Engineering, Aalto University, Kemistintie 1, Aalto 00076, Finland

© The Minerals, Metals & Materials Society 2019
G. Lambotte et al. (eds.), *Materials Processing Fundamentals 2019*, The Minerals, Metals & Materials Series, https://doi.org/10.1007/978-3-030-05728-2_21

Introduction

Today, oxy-fuel combustion is considered as one of the major technologies for CO₂(gas) capture in power plants. A number of recent studies have also shown its potential to reduce NO_x(gas) and SO₂(gas) emissions. To control and optimize the emission reduction mechanisms, the development of oxy-sulfate thermodynamic database for the oxy-fuel combustion processes is essential. Therefore, the focus of this research is on the thermodynamic modelling of the FeO_x–FeSO₄–Fe₂(SO₄)₃ system with the FactSage 7.2 software package as a part of the larger database of the CaO–MgO–Al₂O₃–SiO₂–FeO–Fe₂O₃–sulfate system.

In the present work, thermodynamic data of FeSO₄ and Fe₂(SO₄)₃ were compiled and critically assessed below 2000 K to obtain accurate thermodynamic parameters. All calculations were carried out using the FactSage 7.2 thermochemical software [1], including the pure substances and self-developed databases.

Phase Relations in the Ternary Fe–S–O System

Recently, the relatively well known Fe–O and Fe–S systems were reevaluated by Hidayat et al. [2] and Walder and Pelton [3], respectively. The ternary Fe–S–O system was investigated by Shishin et al. [4]. In this system, only two stable ternary compounds, FeSO₄ and Fe₂(SO₄)₃ were reported. At ambient pressure conditions, both ternary phases decompose below 1500 K to form the gas and oxide phases before melting [4]. Chemical structures of the anhydrous ferrous sulfate (FeSO₄) and ferric sulfate (Fe₂(SO₄)₃) are illustrated in Fig. 1. Barany and Adami [5], Pankratz and Weller [6] and Majzlan et al. [7] measured the thermodynamic properties of Fe₂(SO₄)₃, and Moore and Kelly [8] measured the low temperature thermodynamic properties of FeSO₄. Using the susceptibility measurement technique, Frazer and Brow [9] and Kirfel et al. [10] measured magnetic data (μ_B) for α-FeSO₄ and β-FeSO₄ to be 4.1 ± 0.4 and 5.44 ± 0.27, respectively.

The anhydrous iron (III) sulfate (Fe₂(SO₄)₃) crystallizes in two modifications, monoclinic and trigonal. The stability relationship between the two phases is not clear. Only the trigonal polymorph has been reported in nature, under the name mikasaite. Mikasaite is formed by precipitation from hot gases escaping fractures in coal beds [7]. Fe₂(SO₄)₃ is rare as a mineral, but it is an important compound for the development of a thermodynamic database for a number of natural hydrated iron sulfates [11] and oxy-fuel combustion applications. More details on the thermodynamic properties of the phases in the FeO_x–FeSO₄–Fe₂(SO₄)₃ system are presented and discussed in the subsequent sections.

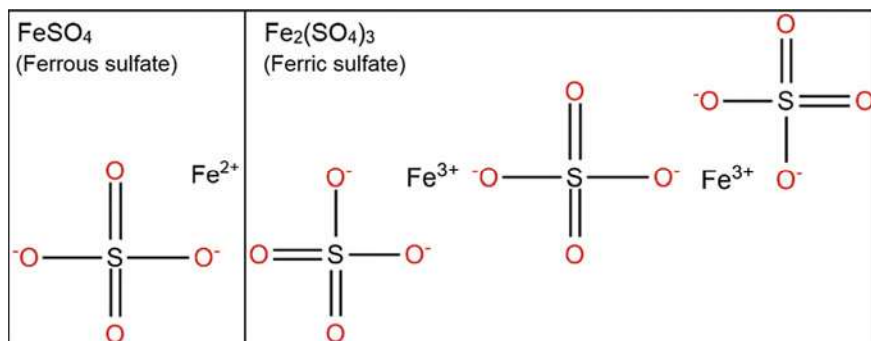
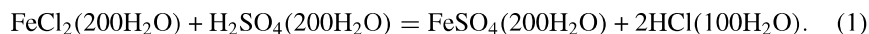


Fig. 1 Schematic diagram of the chemical structures of the ferrous and ferric sulfates, adopted from Chase [13]

Thermochemical Data of FeSO_4 and $\text{Fe}_2(\text{SO}_4)_3$

Enthalpy of Formation (ΔH_f°) of FeSO_4

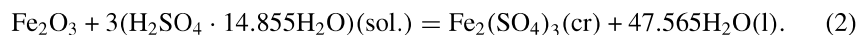
Thomsen [12] measured the enthalpy of Reaction (1). In the NIST-JANAF thermochemical table [13], this enthalpy of Reaction (1) was used to estimate $\Delta_f H^\circ(298.15 \text{ K}, \text{FeSO}_4) = -924.66 \text{ kJ mol}^{-1}$.



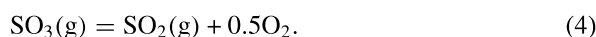
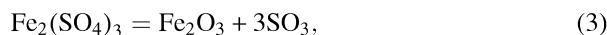
In the NIST-JANAF thermochemical data [13], $\Delta H_f^\circ(298.15 \text{ K}, \text{FeSO}_4)$ values from the decomposition pressure of FeSO_4 reported by D'Ans [14], Greulich [15], and Neumann and Heintke [16] were also estimated by the second and third laws with an average value of $-925.1 \text{ kJ mol}^{-1}$. $\Delta H_f^\circ(298.15 \text{ K}, \text{FeSO}_4) = -928.85 \pm 8.4 \text{ kJ mol}^{-1}$ and $\Delta H_f^\circ(0 \text{ K}) = -919.33 \pm 8.4 \text{ kJ mol}^{-1}$ are the values recommended by Chase [13].

$\Delta H_f^\circ(\text{Fe}_2(\text{SO}_4)_3)$

Based on the data reported for the chemical Reaction (2) by Barany and Adami [5] and using enthalpies of formations of the other components involved in the reaction, $\Delta H_f^\circ(298.15 \text{ K}, \text{Fe}_2(\text{SO}_4)_3) = -2583 \pm 1.7 \text{ kJ mol}^{-1}$ was estimated and presented in [13].



The equilibrium pressures for decomposition of $\text{Fe}_2(\text{SO}_4)_3$ have been determined by several investigators [16–23] at different temperatures via chemical Reactions (3) and (4). The data were critically reviewed by Kellogg [24].



The measured pressure of the chemical equilibrium is the total pressures of $P(\text{SO}_3)$, $P(\text{SO}_2)$, and $P(\text{O}_2)$. In order to calculate the enthalpy change of Reaction (3), the partial pressures of $\text{SO}_3(\text{g})$ from the total vapor pressure data at each temperature was evaluated. Based on the derived values for $P(\text{SO}_3)$, $\Delta H_f^\circ(298.15 \text{ K}, \text{Fe}_2(\text{SO}_4)_3)$ values were derived using the third law and presented in the NIST-JANAF thermochemical data [13]. These average values of the calculations give $-2584.164 \text{ kJ mol}^{-1}$. This value is higher only by $\sim 1 \text{ kJ mol}^{-1}$ than the value they obtained through the data of Barany and Adami [5].

After experimental studies in the temperature range of 273–395 K, Majzlan et al. [7] determined $\Delta H_f^\circ(298.15 \text{ K}, \text{Fe}_2(\text{SO}_4)_3) = -2585.2 \pm 4.9 \text{ kJ mol}^{-1}$, which is higher by $\sim 2 \text{ kJ mol}^{-1}$ than the value of Barany and Adami [5].

Heat Capacity (C_p) and Entropy (S°)

FeSO₄

The low-temperature C_p of the anhydrous FeSO_4 in the temperature range of 53–294.6 K was determined by Moore and Kelly [8] experimentally. Based on standard entropy at 50.12 K, they calculated, $S^\circ(\text{FeSO}_4, 298.15 \text{ K}) = 107.57 \pm 0.84 \text{ J K}^{-1} \text{ mol}^{-1}$. Since the report by Moore and Kelley [8] did not mention the magnetic entropy contribution, an attempt was made by Knacke et al. [25] to add magnetic entropy (S_{mag}) to $S^\circ(\text{FeSO}_4, 298.15 \text{ K})$ and reevaluate the decomposition pressure data. They used the theoretical value of magnetic entropy (S_{mag}) for FeSO_4 $R \ln(2S_{\text{spin}})$, where S_{spin} is the magnetic spin. Since the electrons in the iron ions in FeSO_4 are in a high-spin configuration, they may have used $S_{\text{spin}} = 5/2$ which implies $S_{\text{mag}} = R \ln 5 = 13.4 \text{ J K}^{-1} \text{ mol}^{-1}$. Therefore, the value $S^\circ(298.15 \text{ K}) = (107.57 + 13.4) \text{ J K}^{-1} \text{ mol}^{-1} = 120.96 \text{ J K}^{-1} \text{ mol}^{-1}$ was adopted for FeSO_4 . The C_p above 294.9 K was estimated by comparison with those for MnSO_4 . In the calculations, the high-temperature $C_p(\text{MnSO}_4)$, 870.3–1082.3 K, were taken from the experiments of Southard and Shomate [26].

Fe₂(SO₄)₃

The heat capacities were established by comparison with those for FeSO_4 , assuming their average specific heats, $\text{J K}^{-1} \text{ g}^{-1}$, to be the same. The value of $S^\circ(298.15 \text{ K})$ was estimated so that the second and third law $\Delta H_f^\circ(298.15 \text{ K})$ values, derived from

decomposition pressure data, are in reasonable agreement. The value $S^\circ(298.15\text{ K}) = 120.957 \pm 1.3\text{ J K}^{-1}\text{ mol}^{-1}$ was recommended in the NIST-JANAF thermochemical table [13].

Majzlan et al. [7] studied thermodynamic properties of the monoclinic $\text{Fe}_2(\text{SO}_4)_3$ by acid solution, adiabatic, and semi-adiabatic calorimetry methods. They reported $\Delta H_f^\circ(298.15\text{ K}, \text{Fe}_2(\text{SO}_4)_3) = -2585.2 \pm 4.9\text{ kJ mol}^{-1}$ obtained by an appropriate thermochemical cycle with enthalpies of solution of monoclinic $\text{Fe}_2(\text{SO}_4)_3$, α - MgSO_4 , γ - FeOOH , H_2O , and MgO in 5NHCl and at 298 K . They also compiled C_p values from 0.5 to 400 K and represented the data in the temperature range of 273 – 395 K by Eq. (5).

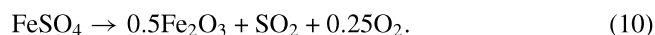
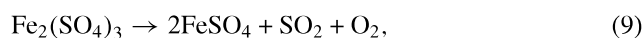
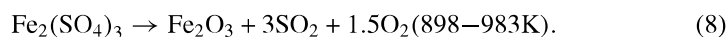
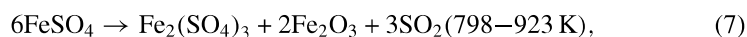
$$C_p/\text{J} \cdot \text{K}^{-1} \cdot \text{mol}^{-1} = 213 + 0.312 \cdot (T) - 2.959 \cdot 10^6 \cdot (T)^{-2}. \quad (273\text{--}395\text{K}) \quad (5)$$

Melting and Decomposition Temperatures

The decomposition temperature 1451 K for $\text{Fe}_2(\text{SO}_4)_3$ at which the total pressure of the gaseous products equals 1 atm , was calculated by [13] through the graphical extrapolation of the decomposition pressure data measured by Warner and Ingraham [27]. By a similar method, they also calculated $T_{\text{decomp.}}(\text{FeSO}_4) = 944\text{ K}$ from the data of Greulich [15]. Reactions (3) and (6) are the decomposition reactions for which the vapor pressure experimental data are available.

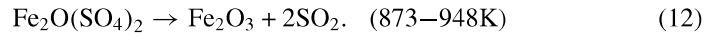


The thermal decomposition of $\text{FeSO}_4 \cdot 6\text{H}_2\text{O}$ was studied by Masset et al. [28] applying the mass spectroscopy coupled with DTA/TG thermal analysis technique under inert atmosphere. After the dehydration, they reported to have observed two decomposition steps for FeSO_4 between 798 and 983 K according to the following Reactions (7) and (8):

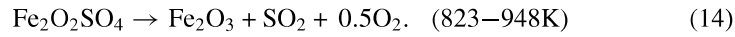
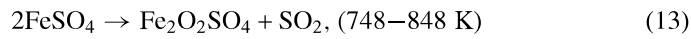


Gallagher et al. [29] studied the thermal decomposition of $\text{FeSO}_4 \cdot x\text{H}_2\text{O}$ using the conventional thermogravimetry, differential thermal analysis, and evolved gas analysis techniques. In an oxidizing atmosphere, they observed that FeSO_4 oxidizes as





In the inert atmosphere



Other proposed decomposition reactions under N_2 (gas) protective atmosphere are for Reaction (7), 891 K [30] (heating rate 20 K/min) and 960 K [31], and for Reaction (3), 951 K [30] (heating rate 20 K/min) and 1028 K [31].

A comparative summary of the decomposition temperatures of FeSO_4 and $\text{Fe}_2(\text{SO}_4)_3$ determined by different researchers and methods are compiled in Table 1.

Table 1 Summary of the phase transition and decomposition temperatures of FeSO_4 and $\text{Fe}_2(\text{SO}_4)_3$

Reaction	$T_{\text{trans.}}/\text{K}$	$T_{\text{decomp.}}/\text{K}$	Ref.	Remark
$\alpha\text{-FeSO}_4 \rightarrow \beta\text{-FeSO}_4$	623	—	[10]	High-pressure phase transition (at $P_{\text{tot}} \approx 15$ kbar)
Reaction (3): $\text{Fe}_2(\text{SO}_4)_3 \rightarrow \text{Fe}_2\text{O}_3 + 3\text{SO}_3$	—	1461	[13]	Determined by the gas pressure measurements of [27]
	—	1017	This work	
	—	951	[30]	Heating rate 20 K min ⁻¹
	—	1028	[31]	—
	—	1024	[7]	—
Reaction (6): $\text{FeSO}_4 \rightarrow \text{FeO} + \text{SO}_3$	—	944	[13]	—
Reaction (7): $6\text{FeSO}_4 \rightarrow \text{Fe}_2(\text{SO}_4)_3 + 2\text{Fe}_2\text{O}_3 + 3\text{SO}_2$	—	798–923	[28]	Inert atmosphere
	—	891	[30]	Heating rate 20 K min ⁻¹
	—	960	[31]	—
Reaction (8): $\text{Fe}_2(\text{SO}_4)_3 \rightarrow \text{Fe}_2\text{O}_3 + 3\text{SO}_2 + 1.5\text{O}_2$		898–983	[28]	Inert atmosphere
Reaction (11): $2\text{FeSO}_4 + 0.5\text{O}_2 \rightarrow \text{Fe}_2\text{O}(\text{SO}_4)_2$ Reaction (12): $\text{Fe}_2\text{O}(\text{SO}_4)_2 \rightarrow \text{Fe}_2\text{O}_3 + 2\text{SO}_2$	—	870–948 873–948	[29]	Oxidizing atmosphere
Reaction (13): $2\text{FeSO}_4 \rightarrow \text{Fe}_2\text{O}_2\text{SO}_4 + \text{SO}_2$ Reaction (14): $\text{Fe}_2\text{O}_2\text{SO}_4 \rightarrow \text{Fe}_2\text{O}_3 + \text{SO}_2$	—	748–848 823–948	[29]	Inert atmosphere

Gibbs Energy Data

The solid gas reactions below 1100 K were studied using the EMF technique by Skeaff and Espelund [32], Hsieh and Chang [33], Musbah and Chan [34], Kobe and Couch [35], Rosenqvist and Hofseth [36], Schaefer [37], in a continuously flowing gas atmosphere, using the vapor pressure measurements technique by Warner and Ingraham [27] and using the DTA technique by Alcock et al. [40]. Gibbs energies of reactions determined by the different methods are summarized in Table 2. These EMF experiments may not correspond to equilibrium with the gas phase, which can contain other gaseous species such as SO_3 , SO_2 and O_2 , but rather to a fixed potential of SO_2 , i.e. the other gaseous species do not form fast enough to significantly change the composition of the flowing SO_2 . If the equilibrium with the gas phase were attained, it would be almost pure SO_2 over the range of P_{O_2} from 10^{-4} to 10^{-14} atm. At higher oxygen potentials, amounts of SO_3 and O_2 become substantial, while at lower P_{O_2} the partial pressure of S_2 starts to increase. The composition of the gas flowing out of the EMF furnaces was estimated by Shishin et al. [4] which indicated that large amounts of condensed phases in EMF cells would have to react in order to produce the gas phase of equilibrium composition, which is not what happened in the experiments.

Jacob and Iyengar [39] studied the $\text{Fe}_2\text{O}_3 + \text{Fe}_2(\text{SO}_4)_3$ phase equilibria by the EMF method. They measured EMF values between 800 and 1000 K. Based on their results, they have concluded that oxysulfates do not form below 1100 K in the Fe–S–O

Table 2 A comparative summary of Gibbs energies of reactions determined by different authors

Equilibrium reaction	$\Delta G_f^\circ (\text{kJ mol}^{-1})$	T/K	Ref.
$\text{Fe}_2(\text{SO}_4)_3 \rightleftharpoons \text{Fe}_2\text{O}_3 + 3\text{SO}_2 + 1.5\text{O}_2$	$970.05 - 0.724 \cdot T$	673–1073	[44]
	$772.32 - 0.724 \cdot T$	920–1020	[32]
	$870.235 - 0.8245 \cdot T$ (± 1.4)	800–1000	[39]
	$704.61 - 0.697 \cdot T$	878–955	[40]
	$802.86 - 0.762 \cdot T$	906–995	[27]
	$753.098 - 0.744 \cdot T$	900–1000	[27]*
	$730.5 - 0.688 \cdot T$	800–900	[43]
$\text{Fe}_2(\text{SO}_4)_3 \rightleftharpoons \text{Fe}_2\text{O}_3 + 3\text{SO}_3$	$576.895 - 0.546.1 \cdot T$ (± 0.5)	800–1000	[39]
	$557.42 - 0.558 \cdot T$	900–1000	[27]*
$\text{Fe}_2(\text{SO}_4)_3 \rightleftharpoons 2\text{FeSO}_4 + \text{SO}_2 + \text{O}_2$	$395.64 - 0.352 \cdot T$	703–904	[32]
$\text{FeSO}_4 \rightleftharpoons 0.5\text{Fe}_2\text{O}_3 + \text{SO}_2 + 1/4\text{O}_2$	$258.74 - 0.202 \cdot T$	773–903	[44]
$\text{FeSO}_4 \rightleftharpoons 0.5\text{Fe}_2\text{O}_3 + \text{SO}_2 + 1/4\text{O}_2$	$203.47 - 0.202 \cdot T$	779–900	[32]

*Re-calculated from the experimental data of Warner and Ingraham [27]

system. The determined Gibbs energies of reactions involving the gases SO_3 , SO_2 , O_2 are compiled in Table 2.

Combining the high-temperature change in enthalpy of reaction $\text{Fe}_2(\text{SO}_4)_3 = \text{Fe}_2\text{O}_3 + 3\text{SO}_2(\text{g}) + 1.5\text{O}_2(\text{g})$ reported by Jacob and Iyengar [39] with the pure substances enthalpy data of FactSage 7.2 for $\text{SO}_2(\text{g})$ and Fe_2O_3 , we have calculated $\Delta H_f^\circ(\text{Fe}_2(\text{SO}_4)_3) = -2586.55 \text{ kJ mol}^{-1}$. This value is higher only by $-1.35 \text{ kJ mol}^{-1}$ than that of Majzlan et al. [7]. Warner and Ingraham [27] have also determined the enthalpy of decomposition of $\text{Fe}_2(\text{SO}_4)_3$ from the vapor pressure measurements to be $\Delta H_{\text{decomp}}^\circ = 566.51 \text{ kJ mol}^{-1}$.

Results and Discussion

The $C_p(\text{SO}_3)$ functions obtained through the reactions $\text{MeO} + \text{SO}_3 = \text{MeSO}_4$ ($\text{Me} = \text{Ca}, \text{Mg}, \text{Mn}$) were calculated by applying the Neumann–Kopp's rule described in Alcock et al. [41]. With the obtained C_p values, the corresponding $C_p(\text{FeSO}_4)$ values were calculated according to Reaction (6). The results are illustrated in Fig. 2.

The heat capacities of FeSO_4 were calculated between 273 and 400 K by comparison with those experimental data reported for $\text{Fe}_2(\text{SO}_4)_3$, assuming their average

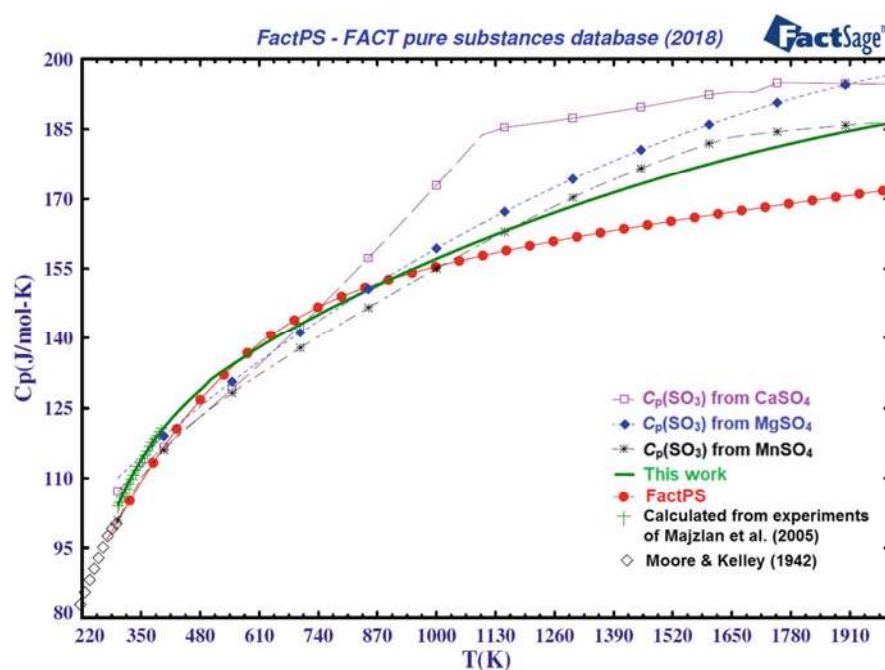


Fig. 2 C_p versus T diagram of FeSO_4

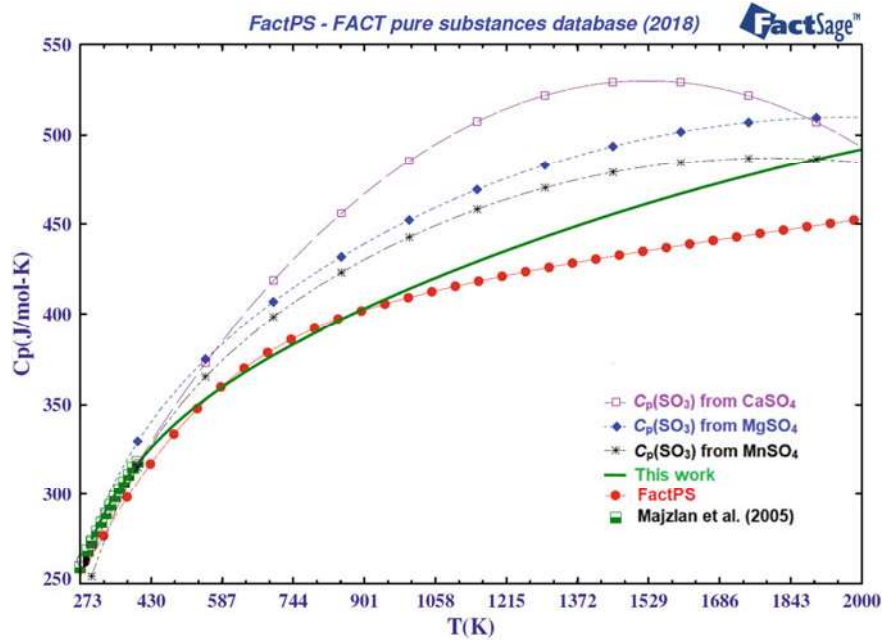


Fig. 3 C_p versus T diagram of $\text{Fe}_2(\text{SO}_4)_3$

specific heats, $c_p(\text{J K}^{-1} \text{g}^{-1})$, to be the same. We have also calculated the experimental $C_p(\text{FeSO}_4)$ values reported by Moore and Kelly [8] for the temperature range 273–295 K. By combining these all C_p values with the $C_p(\text{FeSO}_4)$ obtained through the derived $C_p(\text{SO}_3)$ from the reaction $\text{MnSO}_4 = \text{MnO} + \text{SO}_3$ using the data of Barin Sadakane et al. [42], optimal $C_p(\text{FeSO}_4)$ was calculated at each temperature, in the temperature range of 273–2000 K. By using the normal format for C_p polynomials, we fitted all the data together in two temperature ranges, 273–500 K (Eq. 15) and 500–2000 K (Eq. 16). Likewise, we have calculated $C_p(\text{Fe}(\text{SO}_4)_3)$ and the results are illustrated in Fig. 3. The optimized C_p polynomials for $\text{Fe}(\text{SO}_4)_3$ in the temperature range 273–2000 K is expressed by Eq. (17).

$$C_p(\text{FeSO}_4, 273\text{--}500 \text{ K}) = 118.67 + (0.047) \cdot T - (24.903) \cdot 10^5 \cdot T^{-2} - (5.943) \cdot 10^{-6} \cdot T^2, \quad (15)$$

$$C_p(\text{FeSO}_4, 500\text{--}2000 \text{ K}) = 108.213 + (0.0612) \cdot T - (12.842) \cdot 10^5 \cdot T^{-2} - (10.980) \cdot 10^{-6} \cdot T^2, \quad (16)$$

$$C_p(\text{Fe}_2(\text{SO}_4)_3, 273\text{--}2000 \text{ K}) = 305.363 + (0.136) \cdot T - (62.0743) \cdot 10^5 \cdot T^{-2} - (20.7454) \cdot 10^{-6} \cdot T^2. \quad (17)$$

As shown in Fig. 2, at high-temperatures, the C_p values are remarkably higher than the values currently used in the FactSage 7.2 database, which is based on the NIST-JANAF thermochemical data [13].

Recently, Majzlan et al. [7] determined the change in enthalpies of formations of $\text{Fe}_2(\text{SO}_4)_3$ in the temperature range of 273–395 K. This value is higher by about $-2.2 \text{ kJ}\cdot\text{mol}^{-1}$ than the value recommended by NIST-JANAF [13]. In this work, we adopted the value $\Delta H_f^\circ(298.15 \text{ K}, \text{Fe}_2(\text{SO}_4)_3) = -(2585.2 \pm 4.9) \text{ kJ mol}^{-1}$ reported by Majzlan et al. [7], which was obtained through rigorous experimental studies.

By applying our new database for $\text{FeO}_x\text{--FeSO}_4\text{--Fe}_2(\text{SO}_4)_3$, $\Delta G_r^\circ(T)$ for an equilibrium reaction $\text{Fe}_2\text{O}_3 + 3\text{SO}_2 + 1.5\text{O}_2 \rightleftharpoons \text{Fe}_2(\text{SO}_4)_3$ was calculated in the temperature range of 760–1000 K, in which all the available experimental literature data fall. The obtained result is illustrated in Fig. 4 together with the selected experimental literature data presented in Table 2. Except for the values reported by Sadakane et al. [43] and Alcock et al. [40], the literature values are in agreement with our calculation.

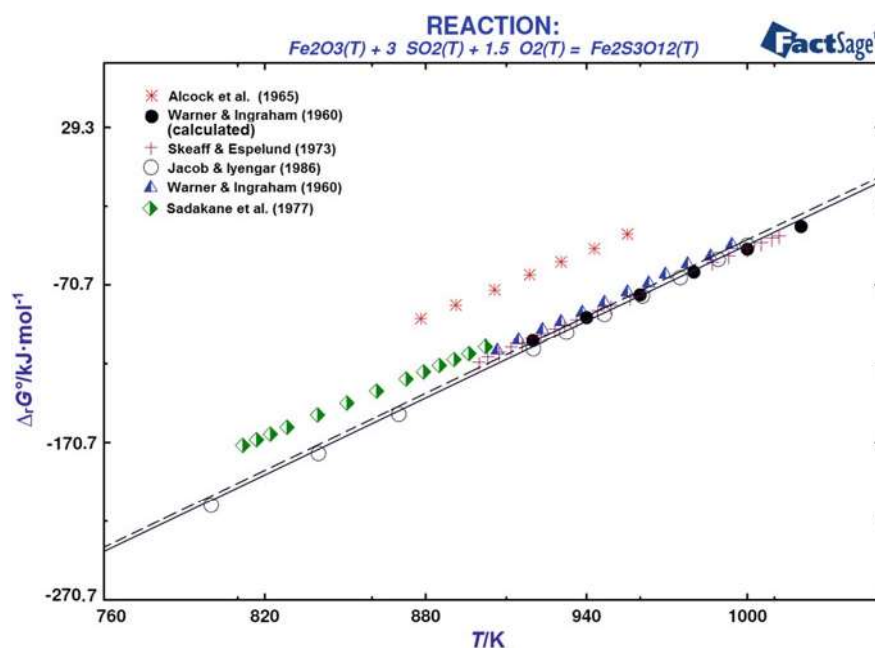


Fig. 4 ΔG_r° versus T diagram for the ferric sulfate formation reaction together with the literature experimental data. The solid line is calculated with the database developed in this work and the dashed line is calculated using the pure substances database in the commercial version of FactSage 7.2 [1]

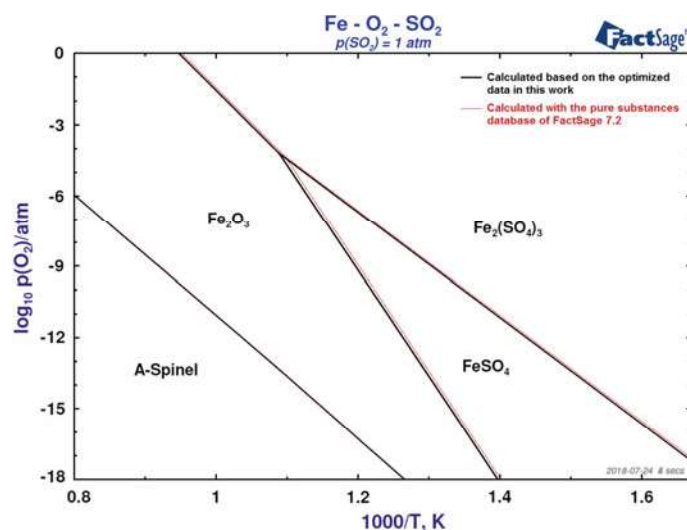


Fig. 5 Calculated potential phase diagram of Fe–O₂–SO₂ at $P(\text{SO}_2) = 1$ atm

Potential Phase Diagrams

Based on the results obtained for FeSO_4 and $\text{Fe}_2(\text{SO}_4)_3$, in this work, and the literature data for the other phases, chemical potential phase diagram has been calculated for the Fe–O₂–SO₂ system between 580 and 1250 K.

The potential phase diagram of $\log_{10} P(\text{O}_2)$ versus T shown in Fig. 5 was calculated at $P(\text{SO}_2) = 1$ atm and $P_{\text{Total}} = 2$ atm. The results obtained are in good agreement with those of Shishin et al.'s [4], hence they may have also used a total pressure close to 2 atm in their calculations.

By graphical extrapolation of the decomposition pressure data measured by Warner and Ingraham [27], we calculated $T_{\text{decomp.}}(\text{Fe}_2(\text{SO}_4)_3) = 1017$ K at which the total pressure of the gaseous products equals one atmosphere. This value is 434 K lower than the value reported in the NIST-JANAF thermochemical data [13] using the same source of experimental data. This large deviation indicates that there were most likely calculation errors in the NIST-JANAF thermochemical data [13]. Our calculations are in agreement with the results reported by [7, 31] and presented in Table 2.

Summary and Conclusions

The development of an oxy-sulfate thermodynamic database for a better understanding and control of SO₂ (gas) emission during oxy-fuel combustion processes is essen-

tial. Therefore, the focus of this research was on the thermodynamic modelling of the iron oxide–sulfate system with the FactSage 7.2 software package. Thermodynamic properties of selected phases in the $\text{FeOx-FeSO}_4\text{-Fe}_2(\text{SO}_4)_3$ system were critically reviewed, compiled and assessed over a wide temperature range of 298–2000 K to obtain accurate thermodynamic parameters. The obtained results were generally in agreement with the literature values in the low-temperature conditions and deviate in the high-temperature conditions. New high-temperature C_p functions, which include the recent experimental data, were optimized. Regarding the decomposition temperatures of FeSO_4 and $\text{Fe}_2(\text{SO}_4)_3$, large deviation were observed among the literature values. This warrants that there is a need for new experiments to accurately determine the decomposition temperatures. According to our assessment of the available literature values, we recommend 944 K for the decomposition of FeSO_4 and 1017 K for the decomposition of $\text{Fe}_2(\text{SO}_4)_3$ according to the reactions $\text{FeSO}_4 \rightarrow \text{FeO} + \text{SO}_3(\text{g})$ and $\text{Fe}_2(\text{SO}_4)_3 \rightarrow \text{Fe}_2\text{O}_3 + 3\text{SO}_3(\text{g})$, respectively, at ambient pressure condition.

Acknowledgements The authors are grateful to the Academy of Finland for financial support. This work was made under the project “Thermodynamic investigation of complex inorganic material systems for improved renewable energy and metals production processes” (Decision number 311537) as part of the activities of the Johan Gadolin Process Chemistry Center at Åbo Akademi University. This work is also a part of the project clean and efficient utilization of demanding fuels (CLUE), with support from the industrial partners: ANDRITZ, Fortum, International Paper, UPM-Kymmene Corporation, and Valmet Technologies Oy.

References

1. Bale CW et al (2009) FactSage 7.2 thermochemical software and databases—recent developments. *Calphad* 33:295–311
2. Hidayat T, Shishin D, Jak E, Decterov S (2015) Thermodynamic reevaluation of the Fe-O system. *Calphad* 48:131–144
3. Walder P, Pelton AD (2005) Thermodynamic modeling of the Fe-S system. *J Phase Equilib Diffus* 26:23–38
4. Shishin D, Jak E, Decterov SA (2015) Critical assessment and thermodynamic modeling of the Fe-O-S System. *J Phase Equilib Diffus* 36:224–240
5. Barany R, Adami LH (1965) Heats of formation of anhydrous ferric sulfate and indium sulfate. *US Bur Mines Rep Invest* 6687:8
6. Pankratz LB, Weller WW (1969) Thermodynamic data for ferric sulfate and indium sulfate. *US Bur Mines Rep Invest* 7280:9
7. Majzlan J et al (2005) Thermodynamics of monoclinic $\text{Fe}_2(\text{SO}_4)_3$. *J Chem Thermodyn* 37:802–809
8. Moore GE, Kelley KK (1942) The specific heats at low temperatures of anhydrous sulfates of iron, magnesium, manganese, and potassium. *J Am Chem Soc* 64:2949–2951
9. Frazer BC, Brow PJ (1962) Antiferromagnetic structure of CrVO_4 and the anhydrous sulfates of divalent Fe, Ni, and Co. *Phys Rev* 125(4):1283–1291
10. Kirfel A, Schafer W, Will G, Buschow KHJ (1977) The high-temperature polymorph $\beta\text{-FeSO}_4$. *Phys Stat Sol (a)* 40:447
11. Hemingway BS, Seal RR II, Chou I.-M (2002) Thermodynamic data for modeling acid mine drainage problems: compilation and estimation of data for selected soluble iron-sulfate minerals. *US Geological Survey Open-File Report*, 02–161

12. Thomsen J (1886) Thermochemische untersuchungen. Verlag von Johann Ambrosius Barth, Leipzig
13. Chase, MW (ed) (1998) NIST-JANAF thermochemical tables. J Phys Chem Ref Data, Monograph No. 9 Part II:959–1951
14. D'Ans J (1905) PhD. dissertation, Darmstadt, Data quoted by B. Neumann and G. Heintke, loc. Cit
15. Greulich E (1927) Z Anorg Chem 168:197–202
16. Neumann B, Heintke G (1937) Z Elektrochem 43:246
17. Keppeler G, D'Ans J (1980) Z Phys Chem 62:89
18. Wöhler L, Plüddemann W, Wöhler P (1908) Eine neue Methode zur Tensionsbestimmung von Sulfaten. Ber Deut Chem Ges 41:703–717
19. Bodenstein M, Suzuki T (1910) Z Elektrochem 16:912
20. Wöhler L, Grünzweig M (1913) Die Sulfat-Tensionen und die Affinität der seltenen Erden. Ber Deut Chem Ges 46:1726–1732
21. Grünzweig M (1913) PhD dissertation, Darmstadt, Germany
22. Blanks RF (1961) PhD dissertation, University of Melbourne, Australia
23. Ingraham TR (1963) Internal Rept. EMT-63-17, Department of Mines and Technical Surveys, Ottawa, Canada
24. Kellogg HH (1964) Critical review of sulfation equilibria. Trans TMS-AIME 230:1622–1644
25. Knacke O, Kubaschewski O, Hesselmann K (1991) Thermochemical properties of inorganic substances, 2nd edn. Springer, Berlin, (KKH 91) pp. 1–1113
26. Southard JC, Shomate CH (1942) Heat of formation and high-temperature heat content of manganous oxide and manganous sulfate. High-temperature heat content of manganese. J Am Chem Soc 64(8):1770–1774
27. Warner A, Ingraham TR (1960) Decomposition pressures of ferric sulphate and aluminum sulphate. Can J Chem 38:2196–2202
28. Masset P, Poinso J-Y, Poignet J-C (2006) TG/DTA/MS Study of the thermal decomposition of $\text{FeSO}_4 \cdot 6\text{H}_2\text{O}$. J Therm Anal Calorim 83:457–462
29. Gallagher PK, Johnson DW, Schrey F (1970) Thermal decomposition of Iron(II) sulfates. J Am Ceram Soc 666–670. <https://doi.org/10.1111/j.1151-2916.1970.tb12038.x>. Accessed 26 July 2018
30. Pannetier G, Bregeault JM, Djega-Maria-Dassou Gerald (1964) Thermal dissociation of ferrous sulfate heptahydrate. C R Acad Sci 258:2832–2835
31. Saflullin NS, Gitis EB, Panesenko NM (1968) Thermochemical transformations of $\text{FeSO}_4 \cdot 7\text{H}_2\text{O}$ during heating in oxidizing and inert media. Russ J Inorg Chem 13:1493
32. Skeaff JM, Espelund AW (1973) An E.M.F. method for the determination of sulphate-oxide equilibria results for the Mg, Mn, Fe, Ni, Cu and Zn systems. Can Metall Q 12:445–454
33. Hsieh KC, Chang YA (1986) A Solid-State Emf Study of Ternary Ni-S-O, Fe-S-O, and Quaternary Fe-Ni-S-O. Metall Trans B 17:133–146
34. Musbah OA, Chang YA (1988) A solid-state EMF study of the Fe-S-O and Co-S-O ternary systems. Oxid Met 30:329–343
35. Kobe KA, JrEJ Couch (1954) Enthalpy-concentration diagram for system ferrous sulfate–water. Ind Eng Chem 46:377–381
36. Rosenqvist T, Hofseth A (1980) Phase relations and thermodynamics of the copper-iron-sulfur-oxygen system at 700–1000 °C. Scand J Metall 9:129–138
37. Schaefer SC (1980) Electrochemical determination of gibbs energies of formation of manganese sulfide and iron sulfide ($\text{Fe}_{0.9}\text{S}$), RI, 8486, Albany Research Center Bureau of Mines, Albany, OR
38. Espelund AW, Jynge H (1977) The zinc-iron-sulfur-oxygen system equilibria between sphalerite or wurtzite, pyrrhotite, spinel, zinc oxide and a gas phase. Scand J Metall 6:256–262
39. Jacob KT, Iyengar GNK (1986) Thermodynamic study of Fe_2O_3 - $\text{Fe}_2(\text{SO}_4)_3$ equilibrium using an oxyanionic electrolyte (Na_2SO_4 -I). Metall Trans B 17:323–329
40. Alcock CB, Sudo K, Zador S (1965) The free energies of formation of the sulfates of cobalt, copper, nickel, and iron. Trans TMS-AIME 233:655–661

41. Tesfaye F et al (2014) Thermal stabilities and properties of equilibrium phases in the Pt-Te-O system. *J Chem Thermodyn* 106:47–58
42. Barin I (1989) Thermochemical data of pure substances, Part II. VCH Verlagsgesellschaft, Weinheim/VCH Publishers, New York
43. Sadakane K, Kawakami M, Goto KS (1977) Measurement of the standard free energy of formation of sulfides and sulfates using oxygen concentration cells with $\text{ZrO}_2\text{-CaO}$. *Tetsu-to-Hagané* 63(3):432–440
44. Turkdogan ET (ed) (1980) Physical chemistry of high temperature technology. Academic Press, New York